

# Impedance Measurement and Selection of Electrochemical Equivalent Circuit of a Working PEM Fuel Cell Cathode

Kazimierz Darowicki<sup>1</sup> · Lukasz Gawel<sup>1</sup> 

Published online: 23 February 2017

© The Author(s) 2017. This article is published with open access at Springerlink.com

**Abstract** The dynamic impedance analysis of direct methanol fuel cell (DMFC) cathode supplied with pure oxygen is presented. Presented results were obtained during dynamic changes of the current density in working fuel cell. Investigation of the occurring processes at cathode was carried with dynamic electrochemical impedance spectroscopy (DEIS). A discussion was conducted based on the determined correlation parameter  $\chi^2$ . It was shown that the selection of an appropriate equivalent circuit cannot be carried out only with correlation parameter of analysis between experimental impedance spectra and the equivalent circuit. Comprehensive analysis of equivalent circuit parameter changes during fuel cell working is needed to determine appropriate equivalent model. Thanks to DEIS technique, comparing of the different equivalent circuits proposed in other works during dynamic changes of operating condition could be presented. In addition, the new electrical circuit has been proposed to describe the cathode performance with poisoned electrocatalyst in fuel cell with reduced efficiency.

**Keywords** DMFC · Cathode · Impedance · DEIS · Equivalent circuit

## Introduction

In the case of proton exchange membrane (PEM) fuel cells, the cathode is the main element that causes voltage drop. To

understand the factors responsible for cathode operation, a range of chemical models were created. Raistrick et al. proposed a thin-film, flooded agglomerate model [1, 2]. In this model, the catalyst layer applied on the surface of an electrochemically neutral substrate is formed by groups of agglomerates that are filled with the catalyst. On the outer side, they are covered with a thin layer of electrolyte. Agglomerates are pushed into open hydrophobic channels. Channel surfaces have a porous structure. The oxidizing agent reaches the porous surface through channels. As a result of diffusion into hydrophobic pores, a gradient of concentrations is formed along the pore.

This model was used in research on electrochemical impedance spectroscopy (EIS) conducted by Ciureanu et al. [3]. It divided the impedance spectrum into three frequency ranges. The membrane filled with conductive ions is represented by the high-frequency part of the spectrum. The catalytic layer of the cathode and processes that occur there are detected in a mid-frequency range. A low-frequency loop seems to be the most interesting as it provides information about diffusion. It is quite important as impedance of cathodic processes is largely determined by transport impedance. This problem has not been presented in an unambiguous manner. A low-frequency range is assigned to slow oxygen diffusion or water diffusion through the membrane or diffusion of generated water through the catalyst layer [4–6].

Apart from the agglomeration model, the thin-layer model proposed by M.S. Wilson, S. Gottesfeld [7] is the one that is considered the most often. In this model, catalyst molecules are deposited in a thin layer of a polymeric membrane.

In the macro-homogeneous model [8], the catalyst layer is treated as a homogeneous matrix of polymeric electrolyte in which the catalyst is deposited, e.g. platinum. This model takes into account the existence of free spaces in polymeric electrolyte.

✉ Lukasz Gawel  
lukasz.gawel@pg.gda.pl

<sup>1</sup> Department of Electrochemistry Corrosion and Materials Engineering, Gdansk University of Technology, 11/12 Narutowicza Street, 80-233 Gdansk, Poland

One of the stages of impedance spectra analysis is selection of an equivalent circuit modelling the tested process. In a further part, the equivalent circuit is correlated with experimental impedance spectra. In this way, numerical values are obtained which electrically characterize the tested physico-chemical process. It does not need to be added that the selection of the equivalent circuit plays a fundamental role in such analysis.

Various equivalent circuits are presented in the literature, which represent processes occurring in the cathode. The first group use numerical models to describe processes [9–11]. Another group includes classical equivalent circuits [12–27]. The diversity of equivalent circuits shows that the selection of one appropriate equivalent circuit that would describe the operation of a cathode in a complete and universal manner is still a big challenge.

The most frequently used basic circuit that is used in the assessment of cathode properties is the Randles equivalent electrical circuit. This circuit is presented in Fig. 1a. An equivalent circuit is used in which the capacity of the double layer is represented by the capacitor [12, 13] and also by a constant-phase element [14–18]. The Randles equivalent circuit contains membrane and electrolyte resistance  $R_\infty$  as well as charge transfer resistance  $R_{CT}$ . Charge-discharge impedance of the electrical double layer is represented by the capacity  $C_{DL}$  or a constant-phase element CPE. The use of the constant-phase element is justified by the porous structure of the cathode and its electrical inhomogeneity. In Randles equivalent circuit, reagent transport is represented by Warburg semi-infinite impedance. Warburg impedance that takes into account a finite diffusion area is also used.

Hosseini and Zardari [19] used a more complex equivalent electrical circuit that is presented in Fig. 1b. In this circuit, apart from the previously defined electric parameters, adsorption resistance  $R_A$  and adsorption capacity  $C_A$  occur. In this way, Hosseini and Zardari took into account the stages of oxygen reduction reactions and the creation of adsorbed

intermediate. The equivalent circuit as proposed by Hosseini and Zadari was used for the assessment of the oxygen reduction process in an alkaline environment by Niya et al. [20] and Mamlouk and Scott [21].

The equivalent circuit proposed by Piela et al. [22], which is presented in Fig. 1c, takes into account two processes occurring on the fuel cell cathode. The first of them is oxygen reduction, while the other one involves the oxidation of methanol permeating through the membrane. The capacity  $C_{DL}$  is the sum of the capacity of the double layer of oxygen reduction process and double layer capacity of oxidation of the methanol transported through membrane. It describes a non-faradaic capacitances of local oxygen reduction capacitance and local methanol reduction of cathode pores. Charge transfer resistance  $R_{CT}$  also consists of these two processes.  $R_O$  and  $L$ , on the other hand, are responsible for the crossover methanol oxidation.

Apart from those listed above, a range of other equivalent circuits can be found which represent the fuel cell cathode [23–27].

A short review reveals that there is no general, universal electric equivalent circuit, which would represent the cathode processes. Each modification of the Randles equivalent circuit takes into account other phenomena, such as the participation of ions other than hydronium ions, the finite diffusion area, the porous surface of the cathode and adsorption of intermediate products. To solve the problem of selecting an appropriate equivalent circuit, selection is also performed by means of minimizing the correlation parameter  $\chi^2$  [28]. This parameter, also called as goodness of fit parameter, is a measure of fitting quality of the equivalent circuit to the experimental spectrum. In other words, it is a numerical measure of reliability of the proposed electrical model. Usually, to calculate of the  $\chi^2$ , Pearson test is used [29]. Unfortunately, this parameter is not the only one which we should considered, when appropriate equivalent circuit is selected. The value of the  $\chi^2$  parameter depends on the range of measuring frequencies and the number of electrical elements building the equivalent circuit. It also depends on the complexity of electrical elements, for example, the constant-phase element  $CPE = Y_o(j\omega)^n$  is always better to minimize the parameter  $\chi^2$  than any other electrical linear element, as capacitor or resistor. Orazem and Tribollet shown statistical method to evaluate when CPE element can be used [30]. The value of the correlation parameter  $\chi^2$  also depends on the quality of experimental measurements. Lasia proposed a statistical method to modelling properly equivalent circuit [29]. However, these methods still do not provide the validity of the proposed circuits if the results do not show the entire spectra of operating changes.

In many cases, in particular, in the case of potentiostatic measurements, it is difficult to keep the stationarity condition of the tested process. Also, non-stationary environment can result in deforming of the impedance data [31]. Nowadays, the

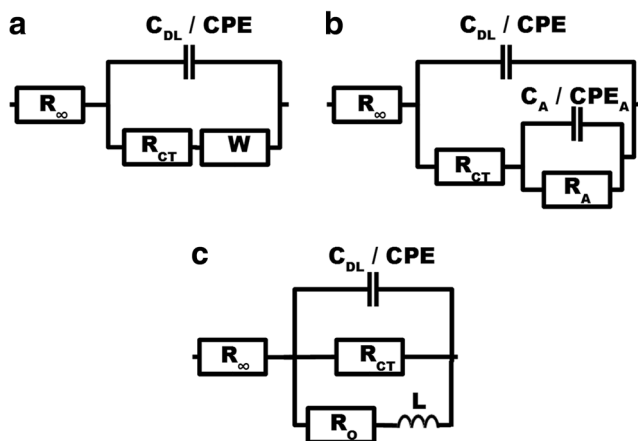


**Fig. 1** a–c Selected equivalent circuits representing a fuel cell cathode

future of the fuel cells is in the use of cars and other objects, which force dynamic changes of the environment, current load, temperature and the others. Therefore, impedance analysis of pseudo-stationary systems may not be sufficient. This implies that finding the right equivalent circuit to describe processes occurring in working fuel cell is not easy. The aforementioned aspects show that the parameter  $\chi^2$  is not the only parameter which should describe the correctness of the selection of an electrical circuit, for this purpose is necessary to analyse full spectra of changes needed. For this reason, changes of the aforementioned equivalent circuit parameters in non-stationary system was presented. Also, new equivalent circuit has been proposed.

## Experimental

A commercial direct methanol fuel cell (DMFC) with an active surface of  $1 \text{ cm}^2$  was used for the experiment. The membrane electrode assembly consisted of Nafion 117 membrane (thickness  $183 \text{ }\mu\text{m}$ ), a cathode from  $4 \text{ mg cm}^{-2}$  Pt on a carbon support and an anode of  $4 \text{ mg cm}^{-2}$  Pt/Ru also on a carbon support. The MEA (membrane electrode assembly) was placed between two graphite plates with  $1 \text{ mm} \times 1 \text{ mm}$  channels with serpentine geometry. The fuel was  $1 \text{ M}$  methanol solution that was provided to the cell using a peristaltic pump (Colepalmer Masterflex L/S) at a rate of  $0.5 \text{ ml min}^{-1}$ . The cathode zone, on the other hand, was supplied with the redundant quantity of oxygen at a flow rate of  $10 \text{ ml min}^{-1}$  using a mass flow controller (Brooks MFC 5850E). A quasi-reference Ag electrode with a diameter of  $0.25 \text{ }\mu\text{m}$  was inserted into the cell to control the cathodic process taking into account the membrane resistance. The measurement was performed at  $338 \text{ K}$  using a temperature controller LIM N1200.

To demonstrate experimental data with the equivalent models, the classical EIS technique was used in the first step. The measurement was performed at a load of  $50 \text{ mA cm}^{-2}$ . The frequency range was  $6.3 \text{ kHz}$  to  $1.1 \text{ Hz}$ .

The dynamic electrochemical impedance spectroscopy technique combined with the linear load change was used for detailed verification of the selection of an appropriate equivalent circuit. Multiple sinusoidal excitations are generated by the PXI-4461 in this same frequency range as previous. The amplitude and the phase shift of components were selected in such a way to ensure that the amplitude of the variable signal response does not exceed the measurement of the  $5 \text{ mV}$  value (peak to peak). This signal was introduced into AUTOLAB 302 N where it was summed with a constant-current signal and then supplied to the tested cell. Using an additional PXI-4462 card, voltage signals were registered between the two covers and between the cathode and the quasi-reference electrode. Owing to the use of the short-time Fourier transform, it was possible to obtain spectra during dynamic changes of fuel

cell parameters. The rate of the cell load change was  $50 \text{ }\mu\text{A/s}$ . The measurement was performed under linear current change conditions from the load  $j = 40 \text{ mA cm}^{-2}$  to the load  $j = 120 \text{ mA cm}^{-2}$ . Impedance spectra was analysed with program ZSimpWin.

## Results and Discussion

### Static Correlation Method for the Selection of an Equivalent Circuit

Figure 2 presents an impedance spectrum determined for the cathode under galvanostatic conditions. The density of the constant current was equal to  $j = 60 \text{ mA cm}^{-2}$ . The number of elementary frequencies was  $n = 20$ . The experimental spectrum determined using the FRA method has a shape of a flattened semicircle. This spectrum was analysed using equivalent circuits presented in Fig. 1.

The results of correlation analysis in the form of values of individual electrical elements and values of the fitting quality parameter are presented in Table 1. The summary includes only electrical elements common for all analysed equivalent circuits. In the analysed equivalent circuits, the following occur:  $R_\infty$ —electrolyte resistance,  $R_{CT}$ —charge transfer resistance and  $C_{DL}$ —electrical double layer capacity or  $Y_o(j\omega)^n$ —non-faradaic constant-phase admittance. Also, relative standard error for individual parameters was shown.

The fitting coefficient parameter  $\chi^2$  is usually the parameter, which determines the selection of the equivalent diagram. It should be noticed that the introduction of the constant-phase element  $CPE(Y_o, n)$  instead of  $C_{DL}$  always leads to a decrease in the value of  $\chi^2$ . On the other hand, the values of the

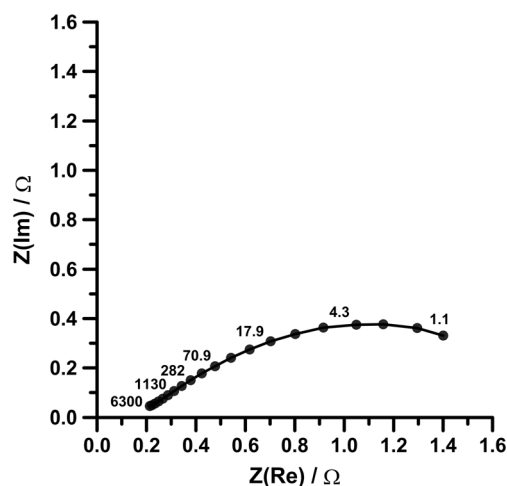


**Fig. 2** A single impedance spectrum of a DMFC cell cathode. The surface of the electrode  $A = 1 \text{ cm}^2$ , the flow rate of the oxygen  $10 \text{ ml min}^{-1}$ , the flow rate of methanol  $0.5 \text{ ml min}^{-1}$ , load  $0.05 \text{ A cm}^{-2}$ , temperature  $338 \text{ K}$

**Table 1** Values of parameters of selected equivalent circuits for a single impedance spectrum with relative standard error (%)

	Equivalent circuit	$\chi^2$	$R_\infty/\Omega$	$R_{CT}/\Omega$	$C_{DL}/\text{mF}$	$Y_0/S\ s^n$	$n$
1a	$R_\infty(C_{DL}(R_{CT}W))$	$2.58 \cdot 10^{-2}$	0.249 (6.41)	0.358 (14.72)	2.73 (18.2)		
1b	$R_\infty(Q(R_{CT}W))$	$3.67 \cdot 10^{-4}$	0.170 (1.95)	2.055 (4.65)		0.144 (5.97)	0.452 (1.94)
2a	$R_\infty(C_{DL}(R_{CT}(C_A R_A)))$	$1.66 \cdot 10^{-2}$	0.239 (5.57)	0.798 (12.04)	2.24 (17.25)		
2b	$R_\infty(Q(R_{CT}(C_A R_A)))$	$1.87 \cdot 10^{-4}$	0.125 (2.03)	1.276 (8.78)		0.142 (3.42)	0.440 (1.61)
3a	$R_\infty(C_{DL}R_{CT}(R_{OL}))$	$8.00 \cdot 10^{-2}$	0.300 (9.21)	0.896 (17.38)	$7.17 \cdot 10^{-3}$ (22.18)		
3b	$R_\infty(QR_{CT}(R_{OL}))$	$9.67 \cdot 10^{-5}$	0.159 (2.57)	3.045 (15.11)		0.193 (8.42)	0.411 (2.36)

exponent  $n$  are lower than 0.5 in all cases. This causes justified doubts. Circuits with two time constants, 2a and 2b, ensure lower  $\chi^2$  values than the Randles circuit 1a and 1b. Equivalent replacement circuits 3a and 3b show the best values of  $\chi^2$  parameters. Using the principle of the minimal  $\chi^2$  value, the equivalent electrical circuit 3b should be selected for the description of the impedance of cathode. However, the value of the constant-phase exponent is lower than 0.5.

Equivalent electrical circuits that contain a constant-phase element show the fitting coefficient at  $\chi^2 \sim (10^{-4}–10^{-5})$ . Circuits that contain the capacity of an electrical double layer  $C$  are characterized by a much lower quality of fitting  $\chi^2 \sim 10^{-2}$ . A lot of processes are approximated using a constant-phase element. In this way, the fitting quality of the proposed model to the experimental results is increased. This is the result from the mathematical characteristics of the constant-phase element. The use of a constant-phase element is not always justified. The CPE influences the value of other electrical parameters, which form the equivalent electrical circuit. For example, the values of resistance  $R_\infty$  decrease considerably depending on the use of the CPE or the  $C$  element. It is hard to determine which values of the parameter are appropriate. Values of the  $\chi^2$  suggest that circuits with CPE are more adequate. Additionally, the determined values of the  $n$  parameter of all circuits fall within the range of 0.4–0.5. It is difficult to justify theoretically such low  $n$  values.

On the basis of the short analysis conducted, we cannot unambiguously justify which of the proposed circuits is the right one that reliably describes processes occurring in the cathode. Each of the proposed equivalent electrical circuits leads to various values of electrolyte resistance, charge transfer resistance and the electrical double layer capacity. Relative standard errors showed that circuits with element CPE have lower values of error of  $R_{CT}$  than circuits with capacitor. Also, the values of the estimated errors showed that values of the individual parameters are different for each circuit. Values of the parameter errors between circuits with CPE are similar. Basing only on the error analysis is not possible to determine appropriate equivalent circuit. Therefore, analysis of the error distribution is insufficient.

To solve this issue, an in-depth impedance analysis must be performed. The dynamic electrochemical impedance

spectroscopy (DEIS) technique was used for this purpose. This method makes it possible to determine changes in the impedance in the function of the selected independence variable. For this purpose, measurements of changes in impedance as a function of constant-current changes were performed. For the in-depth analysis, equivalent electrical circuits containing constant-phase impedance were selected. The main reasons of it were the fact that the fitting coefficient of these circuits was better than the fitting coefficient of circuits including a capacitor by two orders of magnitude. Also, relative standard errors of the parameters in circuits with CPE elements are lower than in circuits with capacitor.

### Analysis of Impedance Changes as a Constant-Current Function

The DEIS technique was used to determine the impedance spectra of the cathode under real operating conditions. This impedance diagram is presented in Fig. 3. Current density was

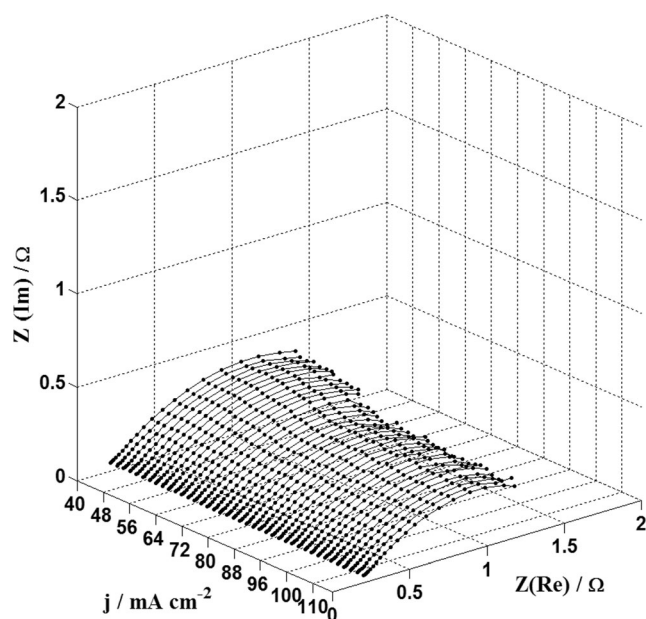


**Fig. 3** The impedance diagram of the cathode of an operating fuel cell at 338 K with a change of load  $50\ \mu\text{A}\ \text{s}^{-1}$ , the oxygen flow rate  $10\ \text{ml}\ \text{min}^{-1}$ , the methanol flow rate  $0.5\ \text{ml}\ \text{min}^{-1}$ , the cathode surface  $1\ \text{cm}^2$



changed linearly within the range of 40 to 110 mA cm<sup>-2</sup>. Each of the elementary spectra has the form of a flattened semicircle. With the load increase, the cathode impedance changes slightly. Only for boundary-level low frequencies is a decrease in the impedance value observed with an increase in the current density.

The obtained impedance diagram was analysed. Individual impedance spectra were analysed using the previously selected equivalent circuits. In this way, relationships were determined for each equivalent circuit between its electrical elements and the current density. At the same time, changes  $\chi^2$  were determined in the current density function as presented in Fig. 4a. The best fitting was obtained for the  $R_{\infty}(QR_{CT}(R_{OL}))$  circuit for which the average value of  $\chi^2 \sim 10^{-5}$ . Additionally, for this circuit, the  $\chi^2$  parameter is weakly dependent on changes in the current density. Thus, the fitting coefficient of this equivalent circuit to impedance spectra is practically constant within

the entire range of impedance spectra. Similar changes in  $\chi^2$  were observed for the two remaining equivalent electrical circuits. For these circuits, however, the fitting quality was much worse. It might seem that the problem of the selection of the most appropriate equivalent circuit has already been solved. But this is very misleading. Apart from the fitting coefficient, changes in individual electrical parameters in the function of current density are also significant for each electrical circuit. The selected equivalent electrical circuits have three parameters in common:  $R_{\infty}$ ,  $R_{CT}$  and CPE( $Y_0$ ,  $n$ ). Therefore, to select the circuit that best represents the experimental results, relationships between these parameters were determined in the direct current function.

Membrane and electrolyte resistance  $R_{\infty}$  changes in the function of current density changes are presented in Fig. 4b. The course of changes in resistance  $R_{\infty}$  for electrical circuits  $R_{\infty}(Q(R_{CT}(C_A R_A)))$  and  $R_{\infty}(QR_{CT}(R_{OL}))$  are practically the

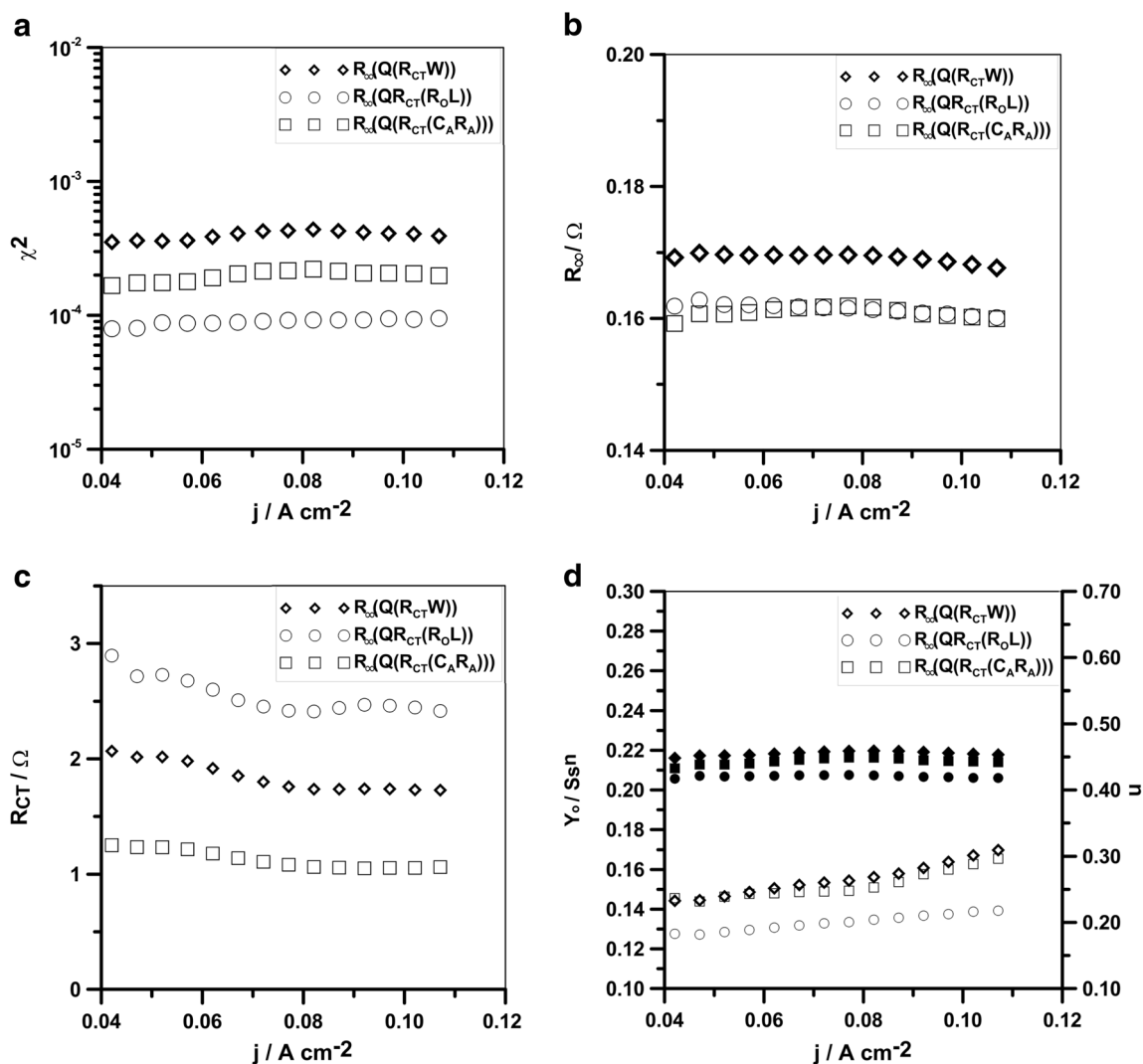


**Fig. 4** Changes of **a** the fitting coefficient parameter  $\chi^2$ , **b** the membrane and electrolyte resistance  $R_{\infty}$ , **c** the charge transfer resistance  $R_{CT}$ , **d** the module  $Y_0$  (unfilled symbols) and the parameter  $n$  (filled symbols) with a change of the current load

same. For the Randles circuit  $R_{\infty}(Q(R_{CT}W))$ ,  $R_{\infty}$  decreases linearly but to a small change with an increase in current density.

In the case of charge transfer resistance, significant differences in the determined values are observed (Fig. 4c). The highest values of  $R_{CT}$  in the entire range of current density correspond to the equivalent circuit  $R_{\infty}(QR_{CT}(R_{OL}))$ , while twice as low values of  $R_{CT}$  correspond to the circuit  $R_{\infty}(Q(R_{CT}(C_A R_A)))$ . The dependence of charge transfer resistance on current density is another issue. In all three cases, charge transfer resistance shows very poor dependence on current density. Such behaviour is contrary to expectations. Theoretically, a strong dependence of  $R_{CT}$  on the current density should be observed.

Non-faradaic admittance is represented by the constant-phase element  $Y_{NF}(j\omega) = Y_0(j\omega)^n$  defined by the exponent  $n$  and the module  $Y_0$ . Figure 4d presents changes in these parameters in the current density function. Modules of constant-phase elements change practically in the same way. The lowest values are reached by the module determined from the equivalent circuit  $R_{\infty}(QR_{CT}(R_{OL}))$ . The highest values correspond to the equivalent circuits  $R_{\infty}(Q(R_{CT}W))$  and  $R_{\infty}(Q(R_{CT}(C_A R_A)))$ . The determined values of exponents  $n$  are constant and independent on the current density. Such behaviour is fully justified. The structure of the electrode, its porosity does not change with the current density change. However, the values of the exponent cause certain doubts. According to the theory presented by De Levie [32], the borderline value of the coefficient  $n$  may not be lower than 0.5. In all cases, the determined values of the coefficients are lower than 0.5 in the entire range of current density.

The presented in-depth impedance analysis shows that each of the analysed equivalent electrical circuits describes processes occurring in the cathode only in a limited way. None of the analysed equivalent electrical models reflect cathodic processes without any objections. It may indicate a reduction of the electrocatalytic properties of cathode. However, it is worth paying attention to the fact that the Randles equivalent electrical model  $R_{\infty}(Q(R_{CT}W))$  consists of the lowest number of electrical elements. This circuit includes Warburg impedance, which models the diffusion process. The other two electrical circuits do not take into account the transport process. For this reason, it was decided that the Randles equivalent circuit should be modified to best reflect processes occurring in the cathode. Modification must cause elimination of the previously presented physicochemical inconsistencies. Additionally, the modification must correspond to physicochemical processes occurring on the cathode.

### Equivalent Electrical Circuit of the Cathode

The electrode in the oxygen flow zone consists of a carbon support with a hydrophobic layer (PTFE), which constitutes a diffusion layer. In the porous layer of the carbon material,

nanoparticles of the catalyst (platinum) are dispersed. Pores are supposed to ensure the even distribution of oxygen to the catalyst surface and easy release of reaction products. The carbon support is not a completely neutral material in the oxygen reduction process [27]. The oxygen reduction process may also occur on the carbon support surface. Especially when materials of tested object have a tendency to ageing or poisoning of the electrocatalyst. Poisoning of the electrocatalyst may result in appearance of the carbon support impedance in impedance spectra. This situation is presented in Fig. 5a. Therefore, the oxygen reduction process occurs over the entire volume, on the surface of the carbon material and on the surface of the platinum catalyst. Oxygen transport takes place in the electrolyte towards reaction surfaces. Therefore, the cathode is a three-dimensional electrode. However, in accordance with the presented model, reaction surfaces can be divided into two parts. One part corresponds to the surface of the catalyst while the other one corresponds to the surface of the carbon material. Reagents are transported in the borderline area. Oxygen reaches to reactive surfaces by means of diffusion through the finite layer with equivalent thickness  $\delta$ . The situation described above is presented in Fig. 5b. The three-dimensional cathode is presented as a two-dimensional model. Both on the surface of the carbon support and on the surface of the catalyst, the following processes occur: discharging and charging of the electrical double layer, the charge transfer process and the oxygen diffusion process through the porous layer with a finite length. Such a model of the oxygen reduction process on a porous carbon electrode with set platinum agglomerates leads to an equivalent electrical circuit presented in Fig. 5c. This circuit is a simple combination of two Randles equivalent circuits. As a result, one part represents the oxygen reduction process on the platinum, the second part represents the oxygen reduction process on the carbon support. The non-faradaic process is represented by the sum of two capacitors. One capacitor represents the capacity of the electrical double layer on the carbon support  $C_{DL C}$ . The other capacitor represents the capacity of the electrical double layer on platinum  $C_{DL Pt}$ . Resistance  $R_C$  and  $R_{Pt}$  corresponds to the charge transfer resistance on the carbon support and on platinum. The charge transfer process on the carbon layer in an oxygen reduction reaction occurs more slowly than on the platinum catalyst. Therefore, the charge transfer resistance on the support  $R_C$  of this process should be relatively high, as compared to the value of charge transfer resistance on platinum  $R_{Pt}$ . The surface of the carbon support layer  $A^C$ , in accordance with the agglomeration model, is higher than the surface of the catalyst  $A^{Pt}$ . As a result, the diffusion process to the catalyst layer is more difficult than in the case of the carbon layer. As a result, processes occurring during oxygen reduction on the carbon support and on the catalyst can be described by simple Randles circuits (Fig. 5b). Diffusion processes were separated in the layer. Transport to the carbon surface through a layer

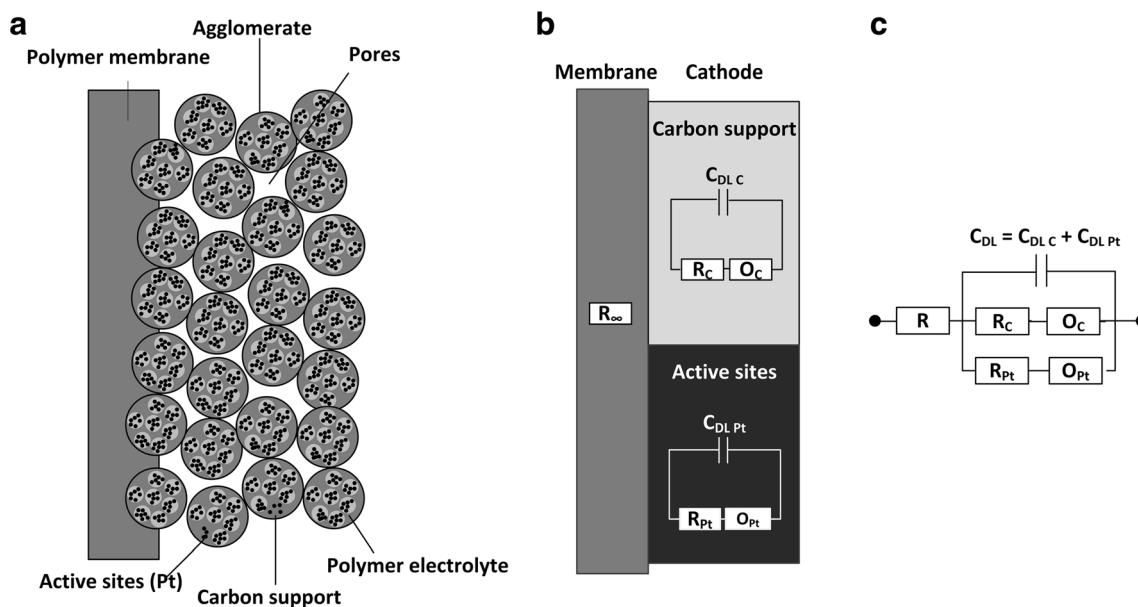


**Fig. 5** The equivalent electrical circuit of an operating fuel cell cathode

with a finite thickness  $\delta_C$  is represented by element O, which can be described with the following impedance (1):

$$Z_C^D(j\omega) = W_C \operatorname{tgh}(B_C \sqrt{j\omega}) \quad (1)$$

Transport to the platinum surface through the layer  $\delta_P$  is represented by the following impedance (2):

$$Z_{Pt}^D(j\omega) = W_{Pt} \operatorname{tgh}(B_{Pt} \sqrt{j\omega}) \quad (2)$$

where  $B_{Pt}/B_C$  is related to finite thickness  $\delta$  and diffusion coefficient  $D$  (3):

$$B = \frac{\delta}{\sqrt{D}} \quad (3)$$

The impedance spectra were analysed on the basis on the equivalent circuit constructed in this way. The results of the analysis were presented in Fig. 6a–f.

Determined values of the correlation coefficient (fitting)  $\chi^2$  within the entire current range are practically constant (Fig. 6a). The average value of this coefficient is  $\chi^2 = 4 \cdot 10^{-5}$ . This shows a very good value of fitting of the circuit to the experimental data, despite the fact that no constant-phase element was used here, which usually simplifies and reduces the fitting coefficient. The membrane and electrolyte resistance  $R_\infty$  decreases slightly with an increase in the current density (Fig. 6b). The charge transfer process in the carbon layer occurs more slowly than on the platinum catalyst. Charge transfer resistance  $R_C$  on the carbon material (Fig. 6d) is two orders of magnitude greater than the value of charge transfer resistance on platinum  $R_{Pt}$

(Fig. 6f). Charge transfer resistance on the carbon material strongly depends on the size of the current density. The resistance  $R_C$  decreases rapidly with an increase in the current load. Charge transfer resistance on platinum behaves in a similar way. The resistance  $R_{Pt}$  decreases rapidly with an increase in the current load. A comparison of resistance values  $R_C$  and  $R_{Pt}$  reveals that charge transfer resistance on active centres is nearly by two orders of magnitude lower than carbon layer resistance, which confirms the previous assumptions. This is related to the rate of the oxygen reduction process, which is much higher on platinum nanoparticles than on active carbon. Exposure of the carbon support may be caused by reduction of electrocatalyst performance of platinum nanoparticles by poisoning.

The Warburg coefficient  $W_{Pt}$  related to the diffusion to the platinum surface decreases linearly together with an increase in the current (Fig. 6e). The parameter  $B_{Pt}$  related to the diffusion layer thickness  $\delta_{Pt}$  does not depend on current density. Impedance  $Z_{Pt}^1$  and  $Z_C^1$  can be described as a sum of charge transfer resistance and diffusion process through the porous layer with a finite length for platinum catalyst (4) and carbon carrier (5).

$$Z_{Pt}^1(j\omega) = R_{Pt}^{ct} + W_{Pt} \operatorname{tgh}(B_{Pt} \sqrt{j\omega}) \quad (4)$$

$$Z_C^1(j\omega) = R_C^{ct} + W_C \operatorname{tgh}(B_C \sqrt{j\omega}) \quad (5)$$

The activity of the platinum catalyst may decrease with the end of lifetime of the fuel cell thanks to poisoning of catalyst. It can reveal the process of oxygen reduction on carbon. Charge transfer resistance of carbon carrier is three orders of magnitude greater than resistance of active sites. Therefore, it can be presumed that Warburg impedance may have the same

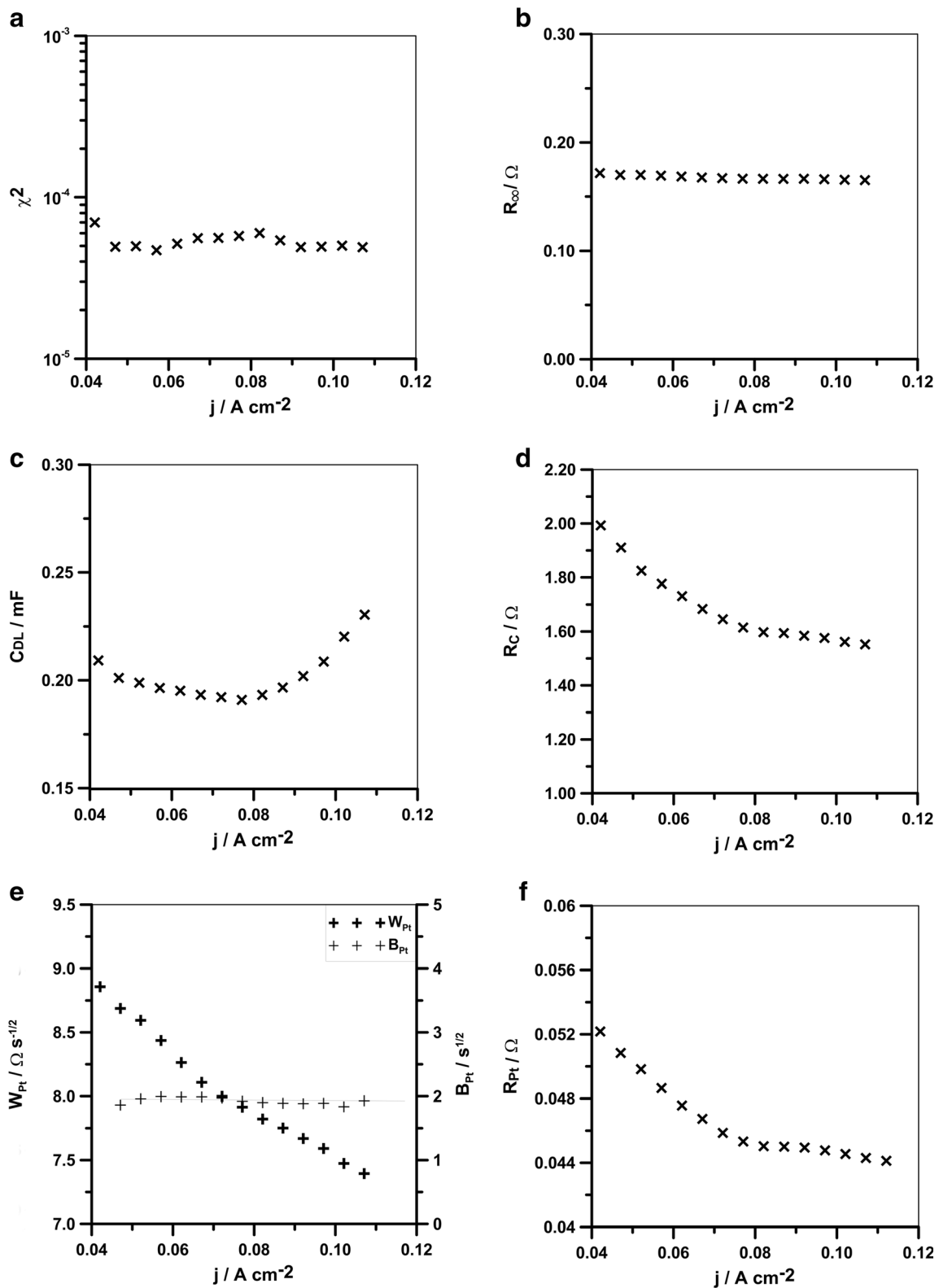


**Fig. 6** Changes of **a** the fitting parameter  $\chi^2$ , **b** the membrane and electrolyte resistance  $R_{\infty}$ , **c** the capacity of the electrical double layer, **d** the charge transfer resistance  $R_C$  on the carbon support, **e** the Warburg

coefficient and the parameter  $B$  related to the diffusion layer thickness and **f** the charge transfer resistance  $R_{Pt}$  on the platinum catalyst with an increase in the current cell load



dependence as charge transfer resistance. Approximately, the Warburg impedance on carbon ( $W_C$ ) should be infinitely higher than the Warburg impedance on platinum ( $W_{Pt}$ ). In summary, Warburg impedance on carbon carrier could not be determined in the analysed range of frequencies. The  $W_C$  values of proposed equivalent circuit tend to infinity. Therefore, we are not able to determine the correct dependence. In this case, the impedance of proposed equivalent circuit on carbon carrier can be simplified to charge transfer process. Also, relative higher ratio of carbon support surface to platinum may be affected.

The ratio of charge transfer resistance of carbon carrier  $R_C$  to charge transfer resistance of catalyst  $R_{Pt}$  may determine the changes of electroactivity of active sites. The electrocatalytic properties of catalyst will be lower if the ratio will be greater. Therefore, catalyst activity will determine the properties of all cathodes. Oxygen reduction reaction is the process which determines the efficiency of working fuel cell. Assuming, the performance of MEA can be determined thanks to compared ratios. Perhaps, it may be possible to determine optimal lifetime of the working fuel cell.

Figure 6c presents a change of the capacity of the double layer. Up to the achievement of a certain current value, the double layer is discharged and next, after the minimum value is reached, an increase in the capacity occurs. This can be induced by a change in the reaction determining the oxygen reduction process, which is followed by a subsequent increase in the capacity on the electrode and an increase in the number of adsorbed particles on the electrode surface.

The use of impedance measurements in the dynamic variant creates additional possibilities for analysis. The selection of an appropriate equivalent electrical circuit is performed at a much higher level of reliability. On the basis of the single analysis, we cannot unambiguously estimate which of the circuits is correct. The CPE used has a positive effect on the value of the quality of fitting of the model to the experimental results. However, the use of a constant-phase element is not always justified. As proved in this study, the CPE influences the value of other electrical parameters, which form the equivalent electrical circuit. The values of resistance  $R_\infty$  change considerably depending on the fact whether we will use the CPE element or  $C$ . Each of the presented circuits leads to various values of individual parameters. It is hard to determine which values of the parameter are appropriate. So far, the selection of the equivalent circuit was based mostly on the correlation coefficient  $\chi^2$ . However, relying only on the parameter  $\chi^2$  is not a correct solution.

In spite of this, relatively low values of the correlation coefficient were obtained. In the analysis conducted using the DEIS technique, circuits proposed in the literature describe processes occurring on the cathode in a limited way. They do not reflect cathodic processes completely and without objections, either. For this reason, the authors proposed their own

equivalent circuit. It includes processes occurring in the platinum catalyst as well as possible processes occurring on the carbon support. Areas described using simple Randles circuits make it possible to interpret changes of individual parameters in a detailed manner. The physicochemical sense of these changes has been retained. It was also possible to achieve a high fitting coefficient despite using a capacity element, which can be assigned to a specific process. Values of charge transfer resistant on the catalyst and on the carbon layer imply that the determining process is the process occurring in the catalytic layer. The capacity of the electrical double layer implies that during the change in the load, a change in the process determines the rate of reduction and an increase in adsorbed particles on the surface of the electrode. The direct influence of crossover on the aforementioned changes is also possible.

## Conclusions

One method of analysis of impedance spectra is the use of an equivalent electrical circuit. Therefore, its selection is of fundamental problem. Correlation coefficient  $\chi^2$  to select an appropriate electrical circuit is not a sufficient criterion. Conducting impedance measurements depending on an independent variable, such as the temperature, changes the potential or the current, making it possible to increase the reliability of the equivalent circuit parameters. The consequence of such an approach to the issue of impedance research is the possibility of analysing changes  $\chi^2$  in the function of the independent variable (in this paper, current is the independent variable). The value  $\chi^2$  should be constant in the entire range of changes of the variable. Additional electrical elements that form the equivalent circuit must have an unambiguous physicochemical meaning. Otherwise, the circuit cannot be used. We cannot obtain this information only from correlation coefficient parameter. In-depth analysis is needed to evaluate changes in circuit parameters. This is possible by using dynamic electrochemical impedance spectroscopy in real working fuel cell in real conditions.

In the case of oxygen reduction on the carbon electrode modified with platinum agglomerates, the equivalent circuit is represented by three elements. The impedance of the first element represents a non-faradaic process characterized by the capacity of the electrical double layer. The impedance of the second element represents impedance of the oxygen reduction reaction on carbon. Impedance of carbon support may be result of poisoned electrocatalyst. The impedance of the third element represents the oxygen reduction process on platinum. The transport process is represented by Warburg impedance in limited space. Therefore, the proposed equivalent electrical circuit is a modification of the Randles equivalent circuit. Attention should be paid to the fact that an appropriately low level of  $\chi^2$  in the entire range of the tested

currents was achieved without the necessity of using a constant-phase element. Additionally, changes in all electrical elements creating the proposed electrical circuit are consistent with theoretical predictions.

**Open Access** This article is distributed under the terms of the Creative Commons Attribution 4.0 International License (<http://creativecommons.org/licenses/by/4.0/>), which permits unrestricted use, distribution, and reproduction in any medium, provided you give appropriate credit to the original author(s) and the source, provide a link to the Creative Commons license, and indicate if changes were made.

## References

1. T.E. Springer, I.D. Raistrick, *J. Electrochem. Soc.* **136**, 1594 (1989)
2. I.D. Raistrick, *Electrochim. Acta* **35**, 1579 (1990)
3. M. Ciureanu, R. Roberge, *J. Phys. Chem. B* **105**, 3531 (2001)
4. T.E. Springer, T.A. Zawodzinski, M.S. Wilson, S. Gottesfeld, *J. Electrochem. Soc.* **143**, 587 (1996)
5. V.A. Paganin, C.L.F. Oliveira, E.A. Ticianelli, T.E. Springer, E.R. Gonzalez, *Electrochim. Acta* **43**, 3761 (1998)
6. N. Wagner, W. Schnurnberger, B. Muller, M. Lang, *Electrochim. Acta* **43**, 3785 (1998)
7. M.S. Wilson, S. Gottesfeld, *J. Appl. Electrochem.* **22**, 1 (1992)
8. C. Marr, X. Li, *J. Power Sources* **77**, 17 (1999)
9. M.S. Kondratenko, M.O. Gallyamov, A.R. Khokhlov, *Int. J. Hydrog. Energy* **37**, 2596 (2012)
10. M. Markiewicz, C. Zalitis, A. Kucernak, *Electrochim. Acta* **179**, 126 (2015)
11. A.A. Kulikovskiy, *J. Electroanal. Chem.* **738**, 130 (2015)
12. T. Schulz, C. Weinmüller, M. Nabavi, D. Poulikakos, *J. Power Sources* **195**, 7548 (2010)
13. J.P. Diard, N. Glandut, P. Landaud, B. Le Gorrec, C. Montella, *Electrochim. Acta* **48**, 555 (2003)
14. S. Cruz-Manzo, R. Chen, *J. Electroanal. Chem.* **694**, 45 (2013)
15. M. Javaheri, *Int. J. Hydrog. Energy* **40**, 6661 (2015)
16. A. Seifitokaldani, O. Savadogo, M. Perrier, *Int. J. Hydrog. Energy* **40**, 10427 (2015)
17. N. Fouquet, C. Doulet, C. Nouillant, G. Dauphin-Tanguy, B. Ould-Bouamama, *J. Power Sources* **159**, 905 (2006)
18. M. Boillot, C. Bonnet, N. Jatroudakis, P. Carre, S. Didierjean, F. Lapique, *Fuel Cells* **6**, 31 (2006)
19. M.G. Hosseini, P. Zardari, *Appl. Surf. Sci.* **345**, 223 (2015)
20. S.M.R. Niya, M. Hoorfar, *J. Electroanal. Chem.* **747**, 112 (2015)
21. M. Mamlouk, K. Scott, *Electrochim. Acta* **56**, 5493 (2011)
22. P. Piel, R. Fields, P. Zelenay, *J. Electrochem. Soc.* **153**, A1902 (2006)
23. W. Zhang, T. Maruta, S. Shironita, M. Umeda, *Electrochim. Acta* **131**, 245 (2014)
24. Y. Fu, S. Poizeau, A. Bertei, C. Qi, A. Mohanram, J.D. Pietras, M.Z. Bazant, *Electrochim. Acta* **159**, 71 (2015)
25. Y. Zhu, W.H. Zhu, B.J. Tatarchuk, *J. Power Sources* **256**, 250 (2014)
26. Y. Wang, G. Liu, M. Wang, G. Liu, J. Li, X. Wang, *Int. J. Hydrog. Energy* **38**, 9000 (2013)
27. D. Qu, *Carbon* **45**, 1296 (2007)
28. B.A. Boukamp, *Solid State Ionics* **10**, 31 (1986)
29. A. Lasia in *Mod. Asp. Electrochem.* vol. 32 ed. By B.E. Conway, J.O. Bockris, R.E. White (Boston, 2002) p. 143.
30. Orazem, M. E. and Tribollet, B. *Assessing Regression Quality, in Electrochemical Impedance Spectroscopy* (New York) p. 385 2008
31. K. Darowicki, P. Ślepski, M. Szociński, *Prog. Org. Coatings.* **52**, 306 (2005)
32. R. de Levie in *Adv. Electrochem. Electrochem. Eng.* vol. 6 ed. By P. Delahay, (New York, 1967) p. 329